Proceedings of the ASME 2013 Fluids Engineering Summer Meeting
FEDSM2013
July 7-11, 2013, Incline Village, Nevada, USA

FEDSM2013-16575

PERFORMANCE AND NEAR-WAKE MEASUREMENTS FOR A VERTICAL AXIS TURBINE AT MODERATE REYNOLDS NUMBER

Peter Bachant*
Department of Mechanical Engineering
University of New Hampshire
Durham, New Hampshire 03824

Martin Wosnik
Department of Mechanical Engineering
University of New Hampshire
Durham, New Hampshire 03824

ABSTRACT

Experiments were performed with a 1 m diameter, 1 m tall three-bladed vertical axis turbine in a towing tank. Rotor power and drag (or thrust) were measured at a tow speed of 1 m/s, corresponding to a turbine diameter Reynolds number $Re_D = 10^6$ and an approximate blade chord Reynolds number $Re_c = \lambda U_\infty c/\nu \sim 10^5$. Mechanical exergy efficiency estimates were computed from power and drag measurements using an actuator disk approach. Characteristics of the turbine's near-wake were measured at one turbine diameter downstream. Variation of all three mean and fluctuating velocity components in the vertical and cross-stream directions were measured at peak turbine power output via acoustic Doppler velocimeter. The effect of tip speed ratio on near-wake mean velocity was observed at the turbine center line. Transverse profiles of mean velocity, fluctuating velocity, and Reynolds stresses were also measured at the turbine's quarter height for two tip speed ratios of interest. Results are compared and contrasted with previous lower Reynolds number studies, and will provide a detailed data set for validation of numerical models.

NOMENCLATURE

η_{II} Mechanical exergy efficiency.
λ Turbine tip speed ratio $\omega R/U_\infty$.
ν Fluid (water) kinematic viscosity.
ω Turbine shaft angular velocity.
ρ Fluid density.
σ Turbine solidity.
A Turbine frontal area.
c Turbine blade chord length.
C_p Turbine power coefficient.
C_d Turbine rotor drag coefficient.
D Turbine diameter.
H Turbine height.
N Number of turbine blades.
R Turbine radius.
Re_c Approximate turbine blade chord Reynolds number.
Re_D Reynolds number based on turbine diameter.
T Turbine shaft torque.
U_∞ Free stream or tow carriage velocity.
U_T Fluid velocity through the turbine when modeled as an actuator disk.

INTRODUCTION

A renewed interest in cross-flow or vertical axis turbines for offshore wind and marine hydrokinetic energy conversion has inspired a push towards advancing understanding and predictive capability for these devices, since they offer some technical advantages compared with horizontal axis turbines. Validating numerical performance models and providing input data to higher level array and environmental models requires detailed measurement of the unique and unsteady flow physics inherent to the operation of these turbines. Furthermore, these models, if they are to be used to design full-scale devices, should in general be checked against experimental data acquired at as close to

*Corresponding author; pxl3@unh.edu

Copyright © 2013 by ASME

TABLE 1. APPROXIMATE BLADE CHORD REYNOLDS NUMBERS $Re_c = \lambda U_\infty c/\nu$ FOR SELECTED TIP SPEED RATIOS.

λ	0.5	1.0	1.5	2.0	2.5	3.0
$Re_c(\times 10^5)$	0.7	1.4	2.1	2.8	3.5	4.2

full-scale as possible, to minimize errors due to the inherently approximate nature of various modeling techniques. Despite the need for larger scale experiments, up until 2006 cross-flow turbine wake data were rare and limited to Reynolds numbers roughly 2-3 orders of magnitude smaller than those seen in full scale devices [1, 2]. Starting in 2006, Ferreira et al. began accumulating much-needed detailed wake data at moderate Reynolds numbers ($Re_c = \lambda U_\infty c/\nu \sim 10^5$) [3, 4], but the available experimental database is still not sufficient. Reynolds number is assumed to have significant effects on the turbine's wake given its effects on static and dynamic performance of airfoils [5, 6]. The effect of Re_c on average power output was shown to be significant on the 2 m Sandia Research Darrieus turbine in wind tunnel testing, where maximum power coefficient increased with Reynolds number, along with a shift of the location of maximum C_p toward lower tip speed ratios due to delayed blade stall [7]. Effects were quite dramatic even over a relatively small range $Re_c = 106,000$–$290,000$. Because a cross-flow axis turbine blade's angle of attack and relative flow velocity varies throughout the turbine's rotation, it is hypothesized that Reynolds number independence for near-wake flow cannot be achieved at typical laboratory scale. It is also hypothesized that Reynolds number differences will have a more noticeable effect in the near-wake, where the features unique to blade performance have not yet been mixed by turbulence [8].

Motivated by the scarcity of data and the disparity between full scale and laboratory experiments, a turbine model and instrumentation system was developed to acquire performance and wake measurements in a towing tank at a turbine diameter Reynolds number $Re_D = U_\infty D/\nu = 10^6$, or an approximate blade chord Reynolds number $Re_c \sim 10^5$. We present both since each should be a relevant driving parameter at their respective scale. Note that calculating true blade chord Reynolds number is not a trivial task, as it varies throughout the turbine's rotation, and this variability is decreased by streamwise induction, hence the definition above. Values of approximate blade chord Reynolds number for selected tip speed ratios are shown in Tab. 1.

Using the newly developed model and instrumentation, the turbine's power and drag (also called thrust) curves were obtained, from which mechanical exergy efficiency—the fraction of the mechanical energy removed from the fluid converted to shaft work—is estimated. This quantity is not commonly assessed for these types of devices, but the method presented here provides an approximate and relatively easy-to-obtain measure of the additional decrease in available mechanical energy downstream due to dissipation during wake recovery, which is relevant to maximizing turbine array performance.

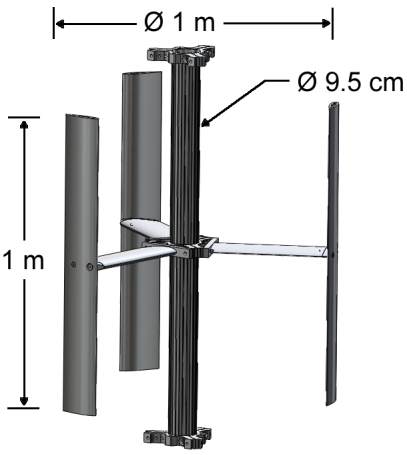

FIGURE 1. TURBINE MODEL DIMENSIONS.

Regarding the turbine's wake, we first set out to obtain a detailed view of the structure and three-dimensionality of the near-wake at optimal operating conditions, i.e. peak power output. Next we wanted to observe the effects of tip speed ratio on the near-wake characteristics, namely variation of center line ($y/R = 0$) mean velocity throughout the entire operating range, and the difference in quarter height velocity profiles between optimum operation and a decreased tip speed ratio, which should increase maximum blade angle of attack, and therefore depth and duration of stall.

EXPERIMENTAL SETUP

Turbine Model

A 1 m diameter, 1 m tall model turbine, shown in Fig. 1, was constructed from three 14 cm chord NACA 0020 blades, resulting in a solidity $\sigma = Nc/\pi D = 0.13$. The blades were fixed at half-chord and mid-span, leaving their tips free. The blade attachment struts were also built from NACA 0020 foils, and fixed to a 9.5 cm diameter shaft.

Experimental Facility and Instrumentation

Experiments were performed in UNH's tow & wave tank, which is 36 m long, 3.7 m wide, and 2.4 m deep. The model turbine had an 11% blockage ratio based on its frontal area. It was installed in a frame built from NACA 0020 struts, mounted to the carriage via linear bearings, allowing a pair of S-beam load cells to measure total streamwise drag. The turbine shaft was loaded with an AC servo motor and gearhead, which provided precise control of turbine tip speed ratio. Shaft torque was measured

Copyright © 2013 by ASME

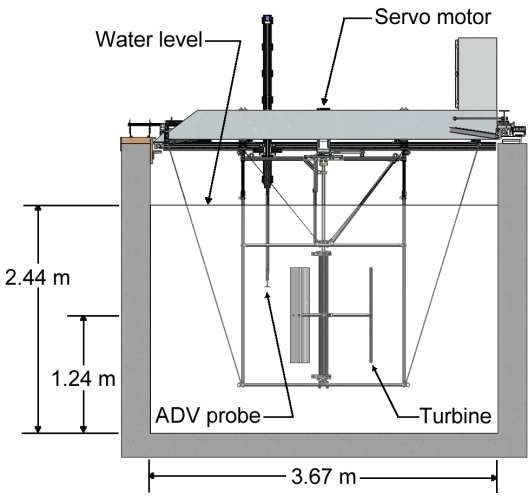

FIGURE 2. FRONT CROSS-SECTION VIEW OF EXPERIMENTAL APPARATUS.

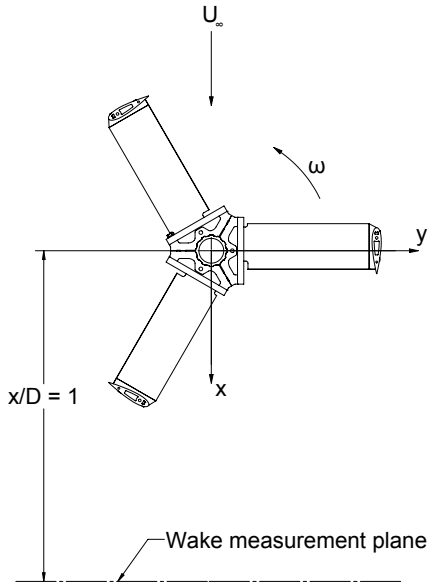

FIGURE 3. TOP VIEW OF TURBINE AND MEASUREMENT COORDINATE SYSTEM.

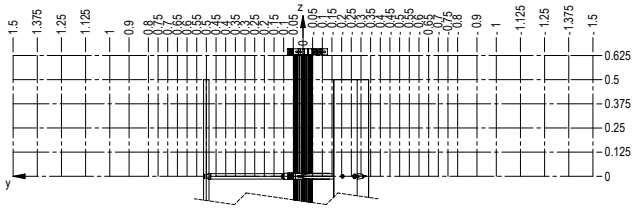

FIGURE 4. FRONT (DOWNSTREAM) VIEW OF TURBINE WAKE MEASUREMENT LOCATIONS. DIMENSIONS ARE IN METERS

with an Interface T8 inline torque transducer mounted between the servo motor and turbine shaft. A schematic of the turbine and instrumentation installed in the tank cross-section is shown in Fig. 2. Signals from the torque transducer and drag load cells were sampled at 2 kHz via National Instruments 9205 and 9237 modules, respectively. Turbine shaft angle was sampled from the servo drive's 10^5 count/rev emulated quadrature encoder output by a National Instruments 9401 counter module.

A Nortek Vectrino+ acoustic Doppler velocimeter (ADV), sampling at 200 Hz, was used to measure wake velocity. The device is capable of measuring all three orthogonal components of velocity simultaneously with an accuracy of $\pm 0.5\%$ its measured value ± 1 mm/s.

Experimental Procedure

The turbine was towed through the tank at 1 m/s, resulting in approximately 17 s of steady turbine operation per run. To ensure repeatability of experimental conditions, minimum standby time between tows was assessed using ADV measurements taken after towing a turbine and returning the tow carriage to its starting position. Turbulence intensity decayed more quickly than low frequency oscillations in the mean streamwise flow, but these were effectively damped by the tank's energy dissipating "beach." From these measurements, a minimum standby time of 4 minutes was chosen.

Tip speed ratio was prescribed and held constant during each tow, ranging from 0.1–3.1. The ADV was mounted on a cross-stream traversing system at 1 turbine diameter downstream ($x/D = 1$) from the turbine axis, the coordinate system for which is shown in Fig. 3. For the power and drag measurements, the ADV was placed at the quarter height $z/H = 0.25$, with $z/H = 0$ corresponding to the turbine center. A duplicate set of measurements were also taken for $z/H = 0$ to show how quarter height and center line measurements differ as a function of tip speed ratio.

After the tip speed ratio $\lambda = 1.9$, corresponding to maximum power output was found, transverse wake profiles were obtained at $z/H = 0$–$\frac{5}{8}$, with a range of $y/R = \pm 3$, shown in Fig. 4. One additional profile was then acquired at $z/H = 0.25$ for the lower-than-optimal tip speed ratio $\lambda = 1.4$.

Turbine power was calculated from the measured torque and angular velocity. Turbine shaft torque was corrected for bearing friction by adding a tare torque, measured in air by driving the turbine shaft with the servo motor. Similarly, drag values were

Copyright © 2013 by ASME

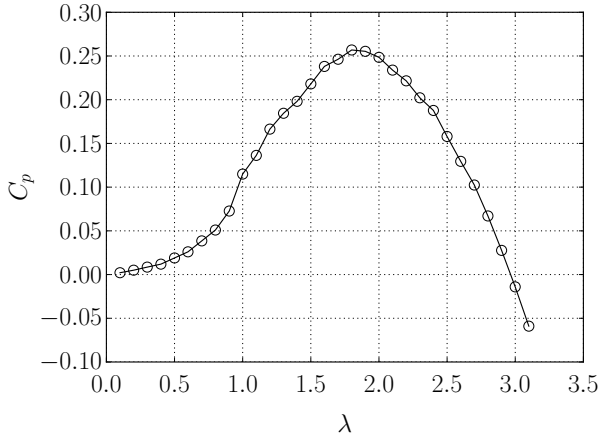

FIGURE 5. TURBINE POWER COEFFICIENT VERSUS TIP SPEED RATIO.

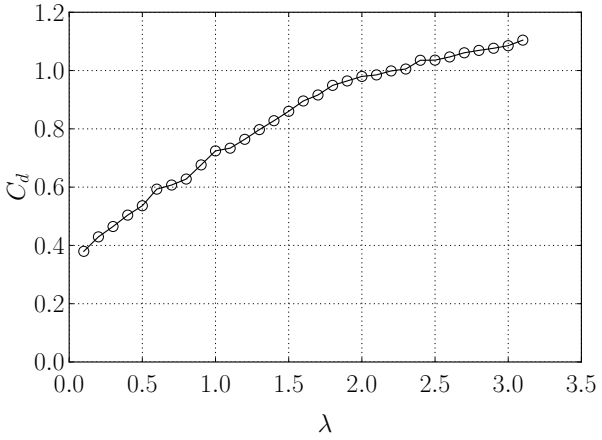

FIGURE 6. TURBINE DRAG COEFFICIENT VERSUS TIP SPEED RATIO.

corrected by subtracting the tare drag, measured by towing the test frame with the turbine removed.

RESULTS AND DISCUSSION

Power, Drag, and Mechanical Exergy Efficiency

Turbine power and drag (thrust) coefficients,

$$C_p = \frac{T\omega}{\frac{1}{2}\rho A U_\infty^3} \tag{1}$$

and

$$C_d = \frac{F_d}{\frac{1}{2}\rho A U_\infty^2}, \tag{2}$$

are shown in Fig. 5 and Fig 6, respectively. Each data point corresponds to a sample mean computed over an integer multiple of blade passages to minimize bias from the periodic nature of the device.

The drag coefficient curve looks as expected—increasing monotonically with tip speed ratio. The power coefficient curve also looks similar in shape to previous experiments with vertical axis turbines [9], reaching a maximum value of 26%.

In order to estimate mechanical exergy efficiency η_{II} of the device, we use the actuator disk approach, i.e. the one-dimensional momentum theory used to derive the Betz limit [10]. This method assumes the power being removed from the fluid by the turbine is equal to the drag force times the flow velocity through the device. Dividing the mechanical power output by rate of change of the fluid's kinetic energy as it passes through the streamtube-bounded control volume, and assuming the inlet and outlet pressures have equalized, we obtain

$$\eta_{II} = \frac{C_p}{(1-a)C_d}, \tag{3}$$

where the induction factor,

$$a = \frac{U_\infty - U_T}{U_\infty}, \tag{4}$$

quantifies the fractional decrease in free stream velocity as it reaches the turbine. For drag coefficients below $8/9$, the induction factor is estimated using the familiar actuator disk solution [10],

$$a = \frac{1-\sqrt{1-C_d}}{2}. \tag{5}$$

For $C_d > 8/9$, the induction factor is estimated using a modified version of the Glauert empirical formula

$$a = \frac{18F - 20 - 3\sqrt{C_d(50-36F)+12F(3F-4)}}{36F-50}, \tag{6}$$

where we assume the tip loss factor $F = 1$ [11]. Using this method, the resulting values of a are approximately a linear function of λ.

To solve for η_{II}, we substitute the estimate for a into Eqn. (3) along with the measured power and drag coefficients. Resulting exergy efficiency estimates are plotted in Fig. 7, reaching a

Copyright © 2013 by ASME

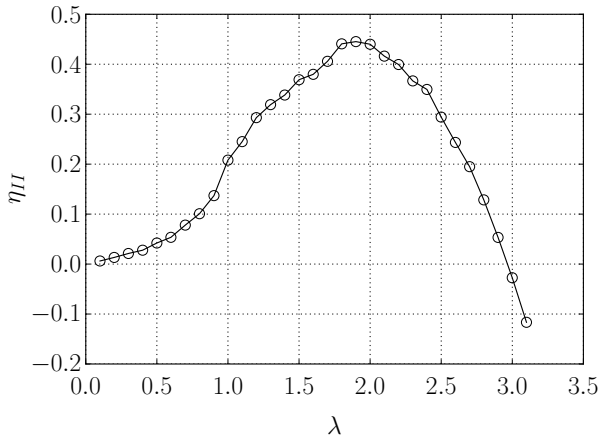

FIGURE 7. TURBINE MECHANICAL EXERGY EFFICIENCY ESTIMATED BY APPLYING ACTUATOR DISK THEORY TO MEASURED POWER AND DRAG COEFFICIENTS.

maximum of 45% at the tip speed ratio corresponding to maximum C_p. This implies that a turbine directly downstream could theoretically extract $\left(1-\frac{C_p}{\eta_{II}} \approx 0.43\right)$ times the power of the upstream, neglecting mixing and entrainment of kinetic energy from the free stream.

Near-Wake Characteristics at Maximum Power Output

Our first goal regarding the wake was to get a detailed picture of what's happening to the flow when the turbine is operating at its peak power output. Similar to the performance measurements, wake velocity statistics were computed over an integer multiple of blade passages. Mean and fluctuating streamwise velocity contours for the turbine operating at $\lambda = 1.9$ are shown in Fig. 8. From these plots we can see the complex asymmetry and three-dimensionality of the wake. We can also see the flow accelerating around the turbine due to blockage. The peak momentum deficit occurs away from the center line at positive values of y/R, while the majority of turbulence intensity occurs around $y/R = -1$, showing evidence of separated flow, possibly due to blades in dynamic stall. Turbulence is found to be approximately locally isotropic, i.e. σ_v and σ_w contours are similar to those of σ_u shown in Fig. 8. A mean streamwise vortex, likely caused by blade end effects, also appears to be passing through the $y/R < 0$ region, as can be seen in the mean v and w velocity components, shown in Fig. 9. The clockwise rotation makes sense considering the blade's suction side faces the inside of its path on the front half of the turbine, and faces outward for the rear half.

Relevant Reynolds stress contours are plotted in Fig. 10. In general, peak values are located in regions of high turbulence in-

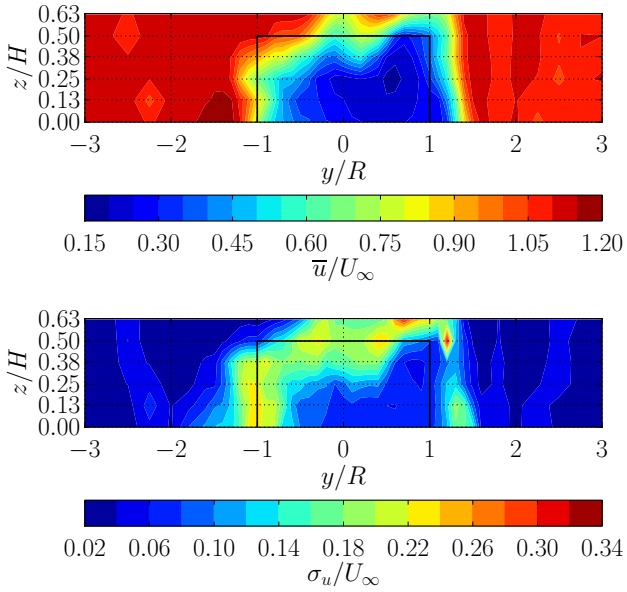

FIGURE 8. CONTOURS OF NORMALIZED STREAMWISE VELOCITY MEAN (TOP) AND STANDARD DEVIATION (BOTTOM) AT $x/D = 1$ AND $\lambda = 1.9$. SOLID BLACK LINES INDICATE TURBINE FRONTAL AREA.

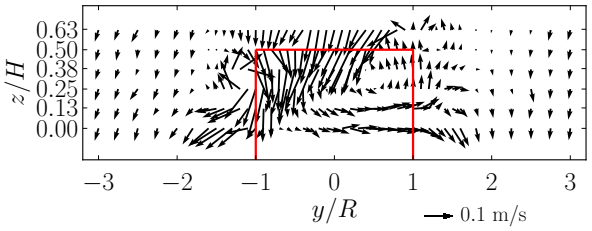

FIGURE 9. MEAN CROSS-STREAM AND VERTICAL VELOCITY COMPONENTS AT $x/D = 1$ FOR $\lambda = 1.9$. RED LINES INDICATE TURBINE FRONTAL AREA.

tensity. It is unclear whether or not we can glean any significant physical intuition from Reynolds stresses so close to the turbine, since periodic forcing from the blades will still play an important role, but at the least Reynolds stresses serve as higher order model validation metrics.

Effects of Tip Speed Ratio on the Near-Wake

From our measurements we can observe how mean velocities at two fixed points downstream of the turbine axis vary with tip speed ratio. These velocity components are shown in Fig. 11. Mean streamwise velocity deficit at at $z/H = 0$ increases with tip speed ratio, which is expected in light of the drag measurements.

Copyright © 2013 by ASME

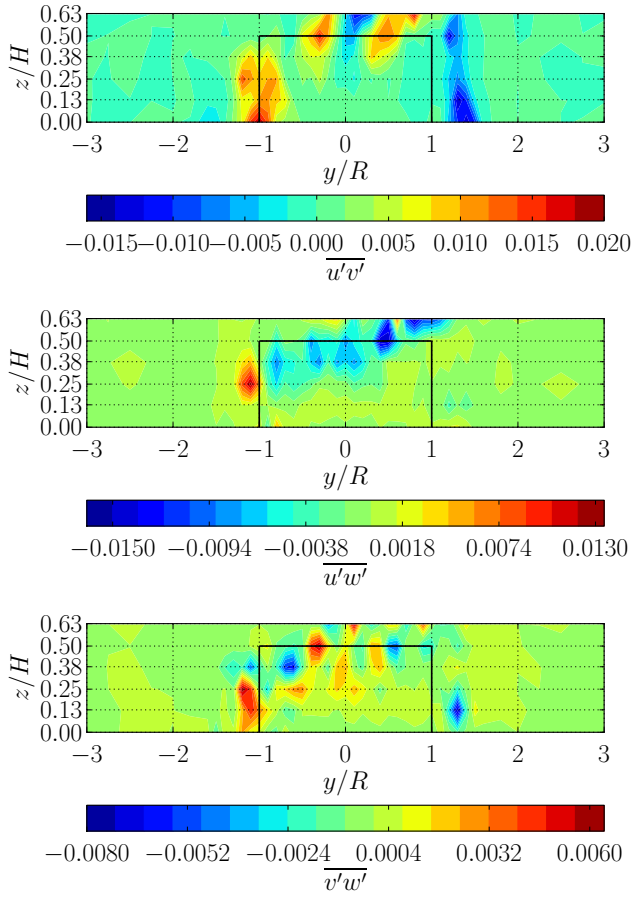

FIGURE 10. REYNOLDS STRESS CONTOURS AT $x/D = 1$ AND $\lambda = 1.9$. SOLID BLACK LINES INDICATE TURBINE FRONTAL AREA.

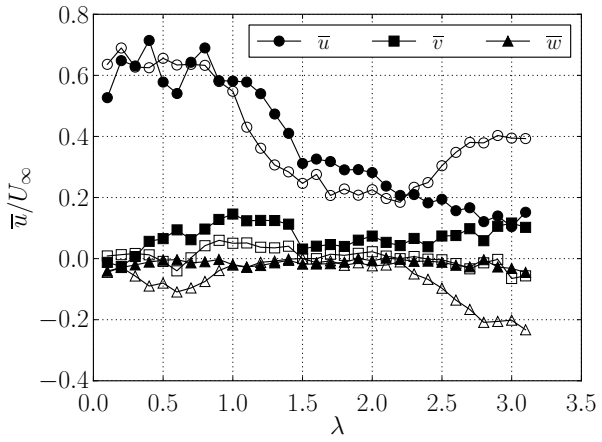

FIGURE 11. NORMALIZED CENTER LINE MEAN VELOCITY COMPONENTS AT $x/D = 1$ VERSUS TIP SPEED RATIO. FILLED MARKERS INDICATE MEASUREMENTS AT $z/H = 0$, WHILE OPEN MARKERS INDICATE MEASUREMENTS AT $z/H = 0.25$.

However, mean velocity deficit at the quarter height is highest at tip speed ratios corresponding to high power coefficient, but decreases at higher values of λ. Mean vertical velocity at the turbine center remains relatively constant across the entire operating envelope, implying the wake is approximately symmetric about $z/H = 0$. However, mean vertical velocity at the quarter height shows a markedly higher downward component at higher λ, corresponding to the similar aforementioned trend of decreasing streamwise velocity deficit at that location. Since drag coefficient continuously increases with λ, we are led to believe the turbine is becoming more like a solid cylinder, letting less flow through, therefore more fluid must flow over the top. Asymmetry about $y/R = 0$ is seen in the mean cross-stream velocity at values of λ away from those of highest power output, with a mean component in the positive y-direction.

Next we want to look more closely at the effects of lowering λ, thereby increasing maximum blade angle of attack and inducing increased stalling behavior. Quarter height streamwise mean velocity profiles for the two tip speed ratios of interest are shown in Fig. 12. Some similarities can be identified with the study by Brochier et al., namely the assymetry of the wake and how its shape changes on the side of the turbine where the blade faces into the flow—positive y for our experiments and negative for theirs [1].

Regarding turbulence intensity in the wake, we can make similar comparisons. The data in Brochier et al. shows two peaks on opposite sides of the turbine axis, with the lower tip speed ratio case having a relatively higher peak on one side [1], which should correspond to negative y values in our case. This is somewhat in agreement with our results, though the value at the origin for our case is relatively higher, which may be due to the larger shaft wake. However, when we compare our two profiles, we notice for the lower value of λ there is higher average turbulence intensity throughout the center region. This appears to be caused by more intense blade stall, beginning earlier along the blade path, i.e. at higher positive values of y. This effect is seen in all three components of turbulence intensity, agreeing with our earlier observations of local isotropy.

Fig. 13 shows mean vertical velocity profiles for the two tip speed ratios of interest. The large gradient appearing at negative values of y, suspected to be the result of blade tip vortices, remains a approximately the same location. However, the peak seen at $y/R = 1.2$ is decreased for the lower tip speed ratio case.

Fig. 14 shows profiles of mean cross-stream velocity. Unlike the streamwise and vertical profiles, these show relatively large differences at our two tip speed ratios of interest, indicating significant fluid motion—on the order of 10% of the free stream

Copyright © 2013 by ASME

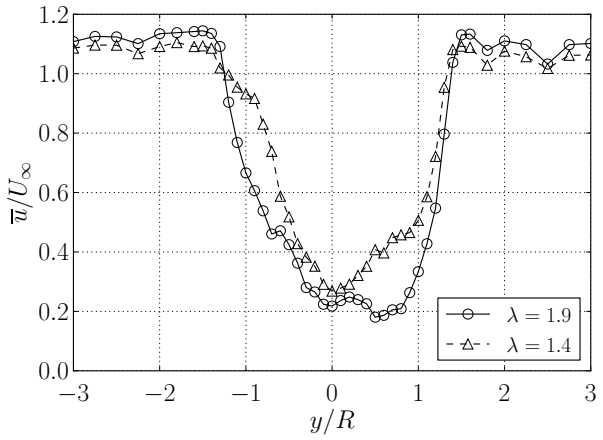

FIGURE 12. STREAMWISE MEAN VELOCITY PROFILES FOR $\lambda = 1.9$ AND $\lambda = 1.4$ AT $x/D = 1$ AND $z/H = 0.25$.

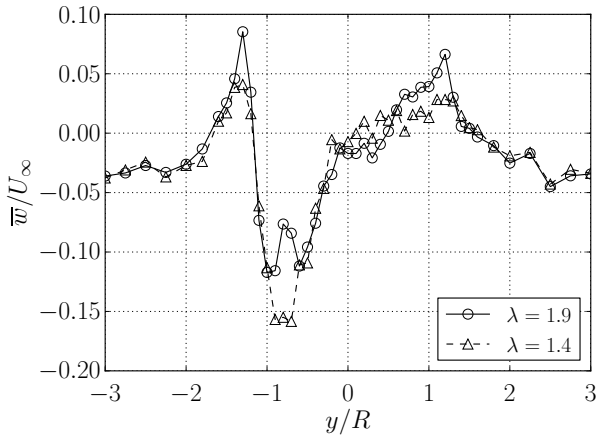

FIGURE 13. MEAN VERTICAL VELOCITY PROFILES FOR $\lambda = 1.9$ AND $\lambda = 1.4$ AT $x/D = 1$ AND $z/H = 0.25$.

velocity—to the left on the left edge of the rotor at $\lambda = 1.9$ and to the right at the right edge of the rotor at $\lambda = 1.4$.

Fig. 16 shows profiles of $\overline{u'v'}$ Reynolds stress. Similar to the profiles of σ_u in Fig. 15, we see a rightward shift of the left peak from what we infer is earlier blade stall, while the right hand peaks are almost identical. In Fig. 17, we see that profiles of $\overline{v'w'}$ Reynolds stress contain peaks once again on the left side of the turbine, but the correlations are opposite for the two tip speed ratios.

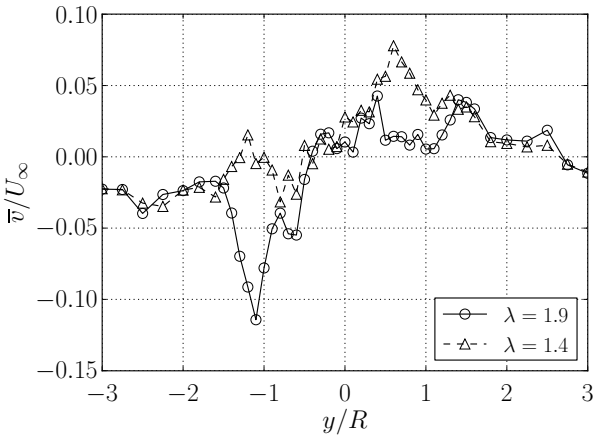

FIGURE 14. MEAN CROSS-STREAM VELOCITY PROFILES FOR $\lambda = 1.9$ AND $\lambda = 1.4$ AT $x/D = 1$ AND $z/H = 0.25$.

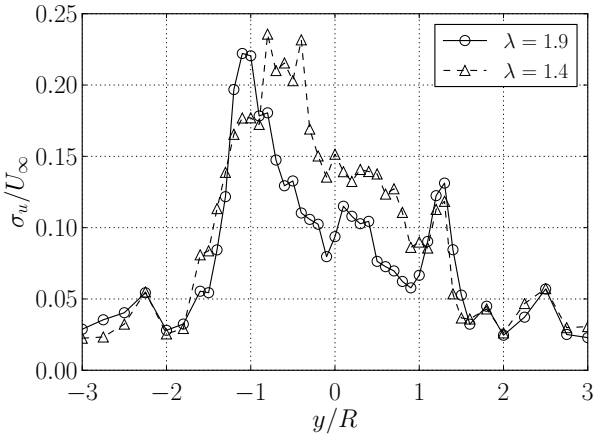

FIGURE 15. STREAMWISE VELOCITY STANDARD DEVIATION FOR $\lambda = 1.9$ AND $\lambda = 1.4$ AT $x/D = 1$ AND $z/H = 0.25$.

CONCLUSIONS

In general, this study was a step towards accumulating detailed performance and wake flow data at increased Reynolds number, which should prove useful in validating turbine performance models and improving accuracy of higher level array or environmental models. This effort will help improve predictive capability of device physics, thereby reducing technical and economic risk.

We presented experimental measurements of power, drag, and near-wake velocity for a vertical axis turbine at moderate Reynolds number, acquired in a towing tank. Drag coefficients increased with λ as expected, reaching a maximum value around 1.1, while power coefficient peaked at 26% at a tip speed ratio of

Copyright © 2013 by ASME

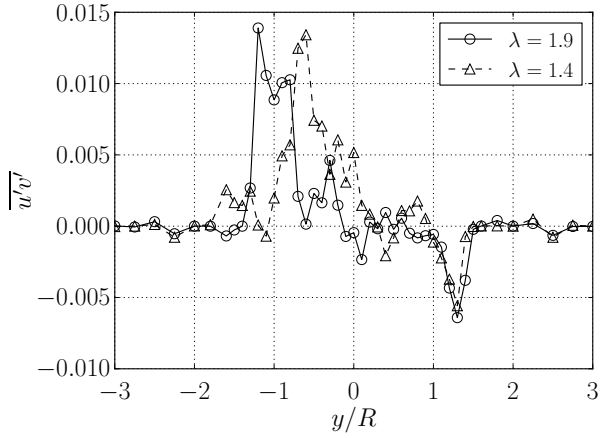

FIGURE 16. $\overline{u'v'}$ REYNOLDS STRESS PROFILES FOR $\lambda = 1.9$ AND $\lambda = 1.4$ AT $x/D = 1$ AND $z/H = 0.25$.

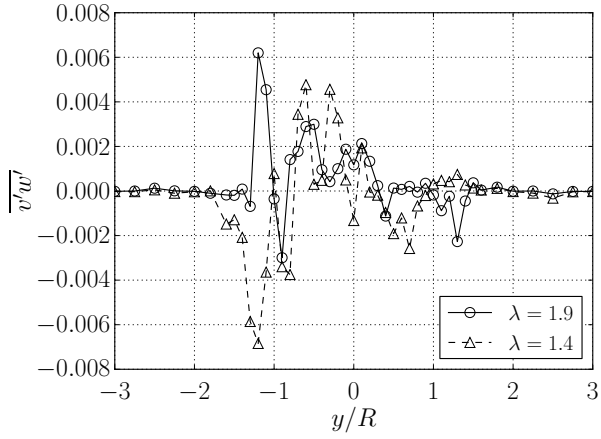

FIGURE 17. $\overline{v'w'}$ REYNOLDS STRESS PROFILES FOR $\lambda = 1.9$ AND $\lambda = 1.4$ AT $x/D = 1$ AND $z/H = 0.25$.

1.8–1.9. Using actuator disk theory combined with the Glauert empirical relation applied to measured power and drag, mechanical exergy efficiency was estimated, reaching a maximum of 45%. This measure provides some insight on the excess fluid energy dissipation of the device when the wake is fully mixed far downstream.

We have investigated the near-wake structure across a relatively large measurement plane at what would be a realistic operating tip speed ratio $\lambda = 1.9$, showing the wake to be highly asymmetric and three-dimensional, shedding what appears to be large streamwise blade tip vortices that show up in the mean flow.

Near wake mean velocity profiles at quarter height show some qualitative agreement with lower Reynolds number 2-D studies, e.g. Brochier et al. and Strickland et al., e.g the change in profile shape when λ was reduced [1, 2]. However, compared with Brochier et al., our turbulence intensity seems to be more spread out over the center region of the turbine, and this effect is increased at our below-optimal tip speed ratio. We attribute this to increased depth and duration of blade stall, caused by an increased maximum blade angle of attack at lower λ.

Regarding future work, despite the wake's complexity it is expected that as the wake evolves downstream, turbine-specific flow structures such as dynamic stall and blade tip vortices will break down and the wake will become better mixed. At some distance—at least in the center plane—we expect the wake to become a fully developed self-similar turbulent plane wake as described by [12]. It is of interest where this will happen, since the wake generated by one turbine will eventually reach a downstream turbine if placed in an array. This will be addressed in future studies, both theoretically and experimentally.

ACKNOWLEDGMENT

The authors would like to acknowledge funding through a National Science Foundation CAREER award (PI Wosnik, NSF-CBET 1150797, program manager Dr. Ram Gupta), and a grant for laboratory infrastructure upgrades from the US Department of Energy.

REFERENCES

[1] Brochier, G., Fraunie, P., Beguier, C., and Paraschivoiu, I., 1986. "Water Channel Experiments of Dynamic Stall on Darrieus Wind Turbine Blades". *AIAA Journal of Propulsion and Power,* ***2***(5), September–October, pp. 46–510.

[2] Strickland, J., Smith, T., and Sun, K., 1981. A Vortex Model of the Darrieus Turbine: An Analytical and Experimental Study. Final report SAND81-7017, Texas Tech University, Lubbock, TX, June.

[3] Ferreira, C., van Kuik, G., van Bussel, G., and Scarano, F., 2006. "Wind Tunnel Hotwire Measurements, Flow Visualization and Thrust Measurement of a VAWT in Skew". *Journal of Solar Energy Engineering,* ***128***, November, pp. 487–497.

[4] Ferreira, C., van Bussel, G., and van Kuik, G., 2009. "Visualization by PIV of dynamic stall on a vertical axis wind turbine". *Experiments in Fluids,* ***46***, pp. 97–108.

[5] Sheldahl, R., and Klimas, P., 1981. Aerodynamic Characteristics of Seven Symmetrical Airfoil Sections Through 180-Degrees Angle of Attack for Use in Aerodynamic Analysis of Vertical Axis Wind Turbines. Final report SAND80-2114, Sandia National Laboratories, Albuquerque, NM, March.

[6] Akbari, M., and Price, S., 2003. "Simulation of dynamic

Copyright © 2013 by ASME

stall for a NACA 0012 airfoil using a vortex method". *Journal of Fluids and Structures,* ***17***, pp. 855–874.

[7] Blackwell, B., Sheldahl, R., and Feltz, L., 1976. Wind Tunnel Performance Data for the Darrieus Wind Turbine with NACA 0012 Blades. Report SAND76-0130, Sandia National Laboratories, Albuquerque, NM, May.

[8] Vermeer, L., Sorensen, J., and Crespo, A., 2003. "Wind turbine wake aerodynamics". *Progress in Aerospace Sciences,* ***39***, pp. 46–510.

[9] Paraschivoiu, I., 2002. *Wind Turbine Design with Emphasis on Darrieus Concept*. Polytechnic International, Montreal, Quebec, Canada.

[10] Manwell, J., McGowan, J., and Rogers, A., 2002. *Wind Energy Explained*. John Wiley, UK.

[11] Buhl, M., 2005. A New Empirical Relationship between Thrust Coefficient and Induction Factor for the Turbulent Windmill State. Technical report NREL/TP-500-36834, National Renewable Energy Laboratory, Golden, CO, August.

[12] George, W., 1989. "The Self-Preservation of Turbulent Flows and Its Relation to Initial Conditions and Coherent Structures". *Advances in Turbulence*, pp. 39–73.

Copyright © 2013 by ASME